

Electromagnetic stress on nucleon structure

Benjamin Koch^{1,2,*}

¹*Pontificia Universidad Católica de Chile
Instituto de Física, Pontificia Universidad Católica de Chile,
Casilla 306, Santiago, Chile*

²*Institut für Theoretische Physik, Technische Universität Wien,
Wiedner Hauptstrasse 8-10, A-1040 Vienna, Austria*

External electromagnetic fields can provoke stress, and thus modifications of the internal structure of nucleons. Working with this hypothesis, one can derive a simple description of the charge dependence of the EMC effect. This first result is confirmed by an explicit model of the structure functions of deformed nucleons in the atomic nucleus.

Contents

I. Introduction	1
II. Expected proportionality in deep inelastic scattering	2
A. General discussion	2
B. EMC effect	2
III. An explicit model of deformed nucleons in the atomic nucleus	4
A. Distribution of deformations in the nucleus	4
B. Edin model for the nucleon	4
C. EMC fit with EMS	5
D. Charge dependence	6
E. Comments	7
IV. Summary	7
References	7

I. INTRODUCTION

Three forces influence the composition, structure, and stability of protons and neutrons (nucleons): The strong force, binding the nucleus together, the weak force, hold responsible for rare weak decays, and the electromagnetic force, typically playing a secondary role. Nucleons contain different types of particles, in particular, quarks carrying charges of all three forces, and gluons propagating the strong force only.

Pictorially, the electromagnetically interacting quarks would swim in a paste of strongly interacting gluons. Even though the electrical charges of some quarks repel each other, the nucleon is held together by the dominant forces of the gluon field $\sim F_{int}$. However, if one would expose this system for example to an external electric field F_{ext} , the quarks would feel this effect directly, while the gluons would feel it only indirectly, through strong interactions with those quarks.

A difference in responding to external electromagnetic forces will necessarily tend to change the spatial composition and even form of the nucleon. This mechanism will be called and abbreviated as Electro-Magnetic Stress (EMS). In a nuclear environment, it is easy to estimate the order of magnitude of this effect. The amount of change in internal structure δ , normalized to $|F_{ext}|/|F_{int}|$, can be expected to be in its order of magnitude quantified by the ratio between the electromagnetic coupling g_e and the strong coupling g_s . Both couplings are scale-dependent, in particular, $g_s = g_s(Q^2)$ can change significantly with Q . Therefore, the ratio δ inherits the Q^2 dependence from the couplings

$$\delta(Q^2) \approx \frac{g_e(Q^2)}{g_s(Q^2)}. \quad (1)$$

Of course, for very high energy processes ($Q^2 \rightarrow \infty$), it is well known that for $g_s(Q^2) \rightarrow 0$ and thus $\delta \rightarrow \infty$. This means that small external electromagnetic fields can change the form of a nucleon completely. This effect is famously known as asymptotic freedom [1, 2]. If, to the contrary, the strong coupling dominates the electromagnetic coupling, all corrections to the form of the nucleon should vanish $\delta \rightarrow 0$, even for strong external electromagnetic fields. However, is this actually the case for small Q^2 ? At very small Q^2 one expects $g_e(0) \approx \frac{1}{137}$ and $g_s(0) \approx \pi$ [3], thus

$$\delta(0) \approx \frac{1}{\pi \cdot 137} \approx 0.002, \quad (2)$$

as an order of magnitude estimate.

Another estimate of this EMS effect can be obtained if one considers the interplay between the positive and the negative electrically charged constituents of a nucleon. Those constituents will be polarized in external electromagnetic fields, which is why this effect is known as “hadron polarizability”. For a review on this topic, see [4]. The corresponding hadronic dipole moment is

$$\vec{p} = 4\pi\alpha_E \vec{E}. \quad (3)$$

In experiments at very low Q^2 and with isolated nucleons, the proportionality factor α_E has been measured to be of the order of $\alpha_E \approx 10^{-3} fm^3$. Between two neighboring

*Electronic address: bkoch@fis.puc.cl

protons, this would correspond to a relative deformation of the proton radius of

$$\delta \sim \frac{\alpha_E}{r_p^3} \approx 0.001, \quad (4)$$

which is in agreement with the estimate (2).

In this article, the testability of changes in the nucleon structure caused by external forces like $F_{ext} \approx qE_{ext}$ will be explored in the context of the EMC effect. In the following section II, deep inelastic scattering will be discussed and a novel application to the puzzling EMC effect (named after the ‘‘European Muon Collaboration’’) will be presented. This argument will be consolidated in section III, where the effect is shown to work with an explicit model for nuclear structure functions. Finally, in section IV, a summary of the results is given.

II. EXPECTED PROPORTIONALITY IN DEEP INELASTIC SCATTERING

A manifestation of the electromagnetic stress on the nucleon structure can be found in the context of Deep Inelastic Scattering (DIS).

A. General discussion

The working hypothesis is that the neutron and proton structure is sensible to the force \vec{F} produced by external electromagnetic fields in the rest frame. If the structure gets modified in one frame, it will get modified in any other frame as well. Thus, also the parton distribution functions f_q summed over the parton content $f = \sum_q f_q$ in the presence of an average external electric $\vec{F}_E \sim \vec{E}q$ and magnetic $\vec{F}_B \sim \nabla(\mu\vec{B})$ forces could be written as

$$f = f(x, \vec{F}_E, \vec{F}_B) \approx f(x, 0) (1 + (\vec{F}_E + g\vec{F}_B + s)d(x)). \quad (5)$$

Please note that the parton model itself is defined for a highly boosted light cone frame but the dependence on external electromagnetic fields is for convenience calculated in the rest frame of the nucleon. Lorentz contraction might lead to different modifications in different directions when going from one frame to another. Thus one has to take the force averaged over the nucleus \vec{F} instead of the local directed force \vec{F} . The correction due to the external fields \vec{F}_E, \vec{F}_B is proportional to $d(x)$ which for small variations around a small x_0 can be approximated to $d(x) \approx d \cdot (x - x_0)$. The constant s summarizes other short range and surface interactions. Here, d, g , and x_0 are the proportionality constants in this linear expansion that will have to be determined experimentally. At leading order, this modification will be reflected one to one if one compares the deep inelastic x -dependent cross-sections of a neutron (proton) with and without external

electromagnetic fields and surface interactions. One finds

$$\begin{aligned} \frac{\sigma(x)_{\vec{F}_E, \vec{F}_B}}{\sigma(x)_0} &\sim \frac{f(x, \vec{F}_E, \vec{F}_B)}{f(x, 0)} \\ &\approx (1 + \vec{F}_E a + (\vec{F}_E + g\vec{F}_B + s)d \cdot (x - x_0)), \end{aligned} \quad (6)$$

where a, g, s, d are proportionality constants. Thus, the x derivative of this ratio is

$$\frac{d}{dx} \frac{\sigma(x)_{\vec{F}_E, \vec{F}_B}}{\sigma(x)_0} \approx \vec{F}_E d + \vec{F}_B g d + ds. \quad (7)$$

B. EMC effect

In the most simple version of an atomic nucleus model, one would expect that the DIS cross-section is given by the cross-section of a nucleon multiplied by the number of participants A (neutrons+protons) in this collision

$$\sigma^{A,Z}(x) = A\sigma^{1,1}(x). \quad (8)$$

Thus, the DIS data for heavy nuclei should be predictable from the DIS data obtained from lighter nuclei and vice versa. In particular, the ratio

$$\Delta_{EMC}^{A,Z} = \frac{\sigma^{A,Z}(x)}{A \cdot \sigma^{1,1}(x)} \quad (9)$$

was expected to be constant (one) and not a function of Bjorken x . The EMC effect, is the famous observation that $\Delta_{EMC}^{A,Z} = \Delta_{EMC}^{A,Z}(x)$ [5]. This observation has triggered numerous experimental tests and theoretical explanations (for a review see, for example [6]). Since the shadowing and anti-shadowing effects of the EMC effect at low $x < 0.2$ are well understood, we will first focus on the linear intermediate regime $0.2 < x < 0.6$. In particular, it was noted that the size of the EMC effect depends on the charge Q of the atomic nuclei [7]. Below, this effect will be studied in the light of our hypothesis of electromagnetic stress acting on nucleons, a perspective which we have not found in the literature.

Let’s return to the most simple version of an atomic nucleus model but allowing for contributions of electromagnetic stress. Larger atomic nuclei will have larger charge Q and thus accumulate larger average electric fields $\vec{E}(Z)$ of the surrounding protons. Therefore, one has to correct the relation (8) by

$$\sigma^{A,Z}(x) = A\sigma_{\vec{F}_E(Z)}(x). \quad (10)$$

In this straightforward model, one can compare the normalized DIS x -dependent cross-section of large nuclei with the DIS cross-section of small nuclei

$$\begin{aligned} \Delta_{\vec{F}}^{A,Z} &= \frac{\sigma^{A,Z}(x)}{A \cdot \sigma^{1,1}(x)} \\ &\approx (1 + (\vec{F}_E(Z) + g\vec{F}_B + s)d \cdot (x - x_0)), \end{aligned} \quad (11)$$

where the expansion point x_0 was chosen to be the point for which this ratio crosses the value of one with a negative slope. For a given isotope, this linear dependence reads $\sim a' + b' \cdot x$. It can be obtained by fitting the experimental data for (11), as shown in figure 1 for the case of an aluminum isotope.

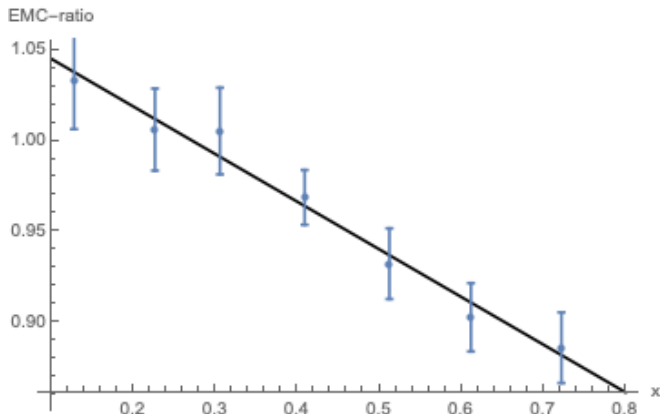


FIG. 1: x -dependence of the ratio (11) for the case of aluminium [7], allowing for a linear fit with $\Delta_{EMC}^{27,13}(x) = (1.07 \pm 0.01) - (0.26 \pm 0.02) \cdot x$, where the given errors are the standard statistical errors of the fit. The fit stops below 0.8, because at higher x the data ceases to be linear and higher orders in $(x - x_0)$ would be necessary fitting this behavior.

This fit was repeated for the elements (*He, Be, C, Al, Ca, Fe, Ag, Au*), using data from [7] and the digitalization tool [8]. For other recent findings on nuclear dependence of the EMC effect see [9–11]. One finds for example that $x_0 = 0.27 \pm 0.02$.

Even more interesting information can be obtained from the x -slope, because it will allow relating to $\bar{F}_E = \bar{F}_E(Z)$. Deriving (11), with respect to x , gives

$$\frac{d}{dx} \Delta_{\bar{F}}^{A,Z} \approx (\bar{F}_E(Z) + g\bar{F}_B + s)d. \quad (12)$$

The magnetic field within the nucleus will be produced by the surrounding spin 1/2 protons and neutrons. However, those are oriented randomly [12] and thus, one can expect the Q dependence of \bar{F}_B in (12) to be subdominant in comparison with \bar{F}_E . The same holds for the short-range contributions s . Let's now estimate the average electric force as a function of nucleon charge $\bar{F}_E \sim q\bar{E}(Z)$ by assuming a constant average charge density ρ . The total charge of such a spherical nucleus is

$$Z = \frac{4}{3}\pi R^3 \rho, \quad (13)$$

which can be solved for the nucleon radius. The radial electric field which is produced by the surrounding protons of a nucleon within the same nucleus is obtained from Gauss law

$$E_r(r) = \frac{1}{\epsilon_0 3} r \rho. \quad (14)$$

The average value of this field is

$$\begin{aligned} \bar{E} &= \frac{1}{\epsilon_0 3} \rho \frac{\int_0^R dr' r'^2 \cdot r'}{\int_0^R dr' r'^2} = \frac{1}{\epsilon_0 4} \rho R \\ &= \frac{1}{\epsilon_0 4} \rho \left(\frac{3Z}{4\rho\pi} \right)^{1/3} \sim Z^{1/3}. \end{aligned} \quad (15)$$

Note that the field (15), produced by the neighboring protons, is the most dominant one. All other contributions, like the field produced by the eventually surrounding electrons or any other external field of the experimental apparatus can be neglected.

Inserting (15) into (12) one obtains a prediction of the charge dependence of the slope data

$$\frac{d}{dx} \frac{\sigma^{A,Z}(x)}{A \cdot \sigma^1(x)} \approx g' + Z^{1/3} d'. \quad (16)$$

The constant g' is expected to originate for example from the largely Z independent average magnetic field \bar{F}_B , or other mean-field and boundary effects. Note that usually the ratio (16) is plotted as a function of atomic number A and not as a function of charge Z . However, this distinction is a subleading effect since A and Z are proportional within the precision of the slopes given here.

The EMC-type ratio has been measured and fitted like in figure 1 for eight different atomic nuclei (*He, Be, C, Al, Ca, Fe, Ag, Au*), which allows extracting the observed data for the predicted charge dependence (16). As shown in figure 2, one gets a good match between (16) and the data obtained from the slope fitting like the one plotted in figure 1. Given the simplicity of the

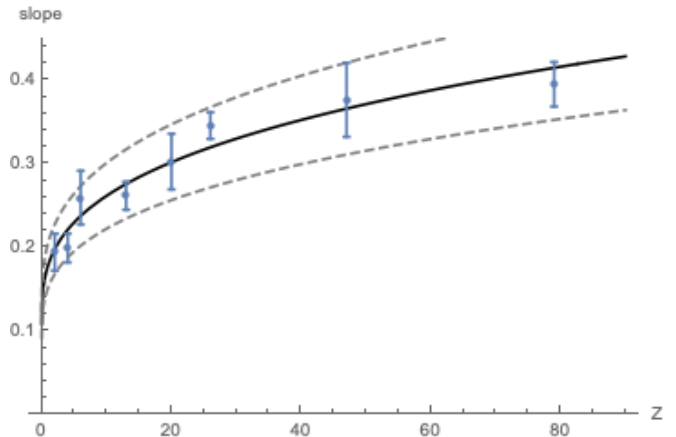


FIG. 2: Charge dependence of (16). The best fit to the experimental data is obtained for $g' = 0.11 \pm 0.02$ and $d' = 0.072 \pm 0.007$. The data points show the statistical error bars of the slope-fits of the ratio (11). The dashed gray lines are an estimate of systematic error of the model (15), which is at least 15% due to the limited validity of the assumption that the charge over mass density ρ is constant for all charges and radii.

underlying idea and model, the good agreement between the model (16) and the data in figure 2 is remarkable.

Note that usually the slope graph 2 is shown as a function of atomic number A and not of atomic charge, but since both quantities are proportional up to 10%, there is no substantial difference between both plots.

III. AN EXPLICIT MODEL OF DEFORMED NUCLEONS IN THE ATOMIC NUCLEUS

A. Distribution of deformations in the nucleus

The difference between stress and “no-stress” can be easily visualized graphically for a toy example. In this example, the toy nucleons within a nucleus all have charge one and are composed of two partons with charge $+1$, one parton with charge -1 , and the electrically neutral but strongly interacting rest, which is confining the nucleon. When neglecting the EM stress, all nucleons shall be described by identical spheres independent of their position within the nucleus, as shown on the left-hand side of figure 3.

This changes when one takes into account the stress felt by the charged partons of an individual nucleon, which is produced due to the “external” electric field of the surrounding nucleons. This stress will tend to pull the negative partons towards the center of the nucleus and push the positive partons towards the outer border of the nucleus and thus deform the nucleon, as shown on the left-hand side of figure 3. Please note that this toy-

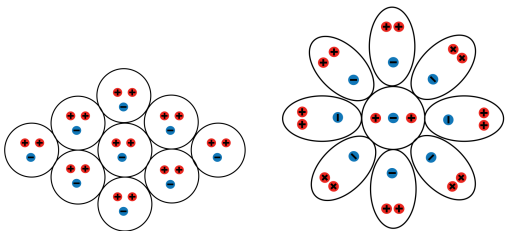


FIG. 3: Toy nucleus without (left) and with (right) EMS

structure 3 is only chosen for illustrative purposes, in order to visualize the EMS mechanism.

The physically relevant question is, whether this electromagnetic stress which was estimated in (2 and 4) is strong enough to be observable in deep inelastic scattering. Apart from the pure size of the deformation, there is an additional effect. In large nuclei, the amount and direction of this deformation will depend on the position of the nucleon within the nucleus, as shown on the right side of figure 3. This dependence, which goes beyond a mean-field approximation, will be considered now.

One expects that the EMS generated deformation is directed radially outward and that its amount increases with distance from the center of the nucleus. For example, the electric field of a spherically symmetric distribu-

tion of constant charge density ρ scales as (14)

$$E_r(r) \sim r\rho.$$

Concerning this, one can distinguish three different regions of deformation within a large nucleus, as shown in figure 4.

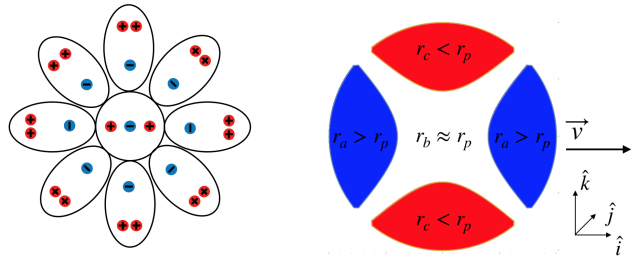


FIG. 4:

Left: Toy nucleus with EM stress.

Right: Nucleon distribution in an atomic nucleus. Nucleons stretched in \hat{i} -direction are indicated with blue, nucleons squeezed in \hat{i} -direction with red, and nucleons with negligible deformation in \hat{i} with white. When integrating the colored volumes in the right figure, one finds that red, white, and blue occupy 54%, 27%, and 19% of the volume. Note that this integration has a rotational symmetry with respect to the \hat{i} direction.

- In the front and back of the nucleus moving with velocity \vec{v} , the thickness in direction \hat{i} is larger than the radius of an undeformed nucleon $r_a > r_p$. This is indicated by the blue region on the right-hand side of figure 4.
- Nucleons in the central part of the nucleus will have negligible stress. The outer nucleons in the diagonal region (e.g. $\sim \pm(\hat{k} \pm \hat{i})$) will be deformed, but their thickness projected on the \hat{i} direction will be approximately the same as the radius of an undeformed nucleon $r_b \approx r_p$. Those cases with $r_b \approx r_p$ are indicated by the white region on the right side of figure 4.
- Nucleons in the lateral belt will be thinner in \hat{i} direction than undeformed nucleons $r_c < r_p$. This is indicated by the red region on the right side of figure 4.

The fraction of nucleons in each of those categories will be labeled p_a, p_b, p_c . If the scattering particle interacts with a long-range interaction, which means it sees the entire nucleus, one expects that $p_a + p_b + p_c = 1$. Further, for a sizeable polarization, one expects the three fractions to be of comparable size, like in figure 4.

B. Edin model for the nucleon

The implications of EMS, which were given above, are intuitive in physical position space. However, structure

functions, relevant for DIS observables, are given in terms of the parton momentum fraction x . To be able to make quantitative predictions about the impact of EMS on DIS one needs a model which describes this transition from position to “ x ” space. For this purpose, we will recur to a description relying on the structure of the Edin model proposed and described in [13, 14]. In this model the dominant contribution to the $F_2^{1,1}$ structure function of the proton takes the form

$$F_2^{1,1}(\tilde{\sigma}, x) = N_p \exp\left(-\frac{x^2}{4\tilde{\sigma}^2}\right) \cdot \operatorname{erf}\left(\frac{1-x}{2\tilde{\sigma}}\right), \quad (17)$$

where the dimensionless parameter $\tilde{\sigma}$ is given in terms of the proton mass m_p and the proton radius r_p measured in the rest frame of the proton

$$\tilde{\sigma} = \frac{1}{r_p m_p} = 0.213. \quad (18)$$

Fitting only one parameter, namely the normalization N_p , one obtains a good fit of the proton structure function, in the x -range, which is relevant for our study, as shown in figure 5. In the following subsections the

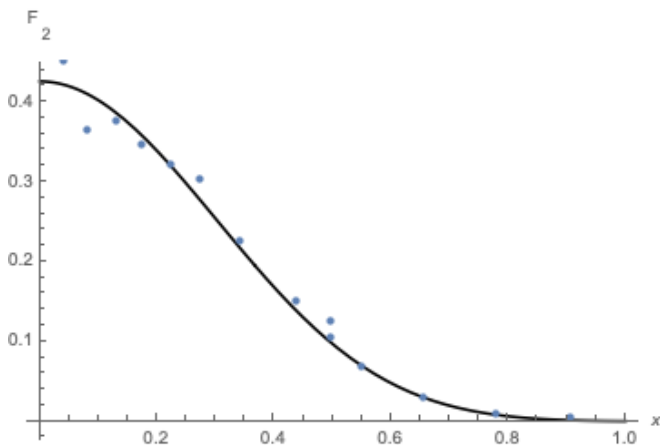


FIG. 5: Fit of the proton structure function $F_2^{1,1}(x)$ at $Q = 15$ GeV [15], using the Edin model (17) and the normalization $N_p = 0.426$.

model (17) will be used to estimate the EMS effects on a nucleus composed of deformed nucleons. In a deformed nucleon, the radius becomes dependent on the direction it is measured. In this case, r_p will refer to the radial direction parallel to the motion of the nucleon as seen from the center of mass frame of the collision measuring this nucleon. The reason for this is that the fractional momentum x is defined in the same direction.

C. EMC fit with EMS

In this subsection, the EMS idea will be implemented in the Edin model (17). This will allow to fit EMC data

from DIS with Iron nuclei. Iron is chosen because it has a very good data quality for large momentum fraction “ x ”.

The EMC effect is typically expressed in terms of a normalized ratio. Let us consider Iron ($A = 56$ and $Z = 26$) and Deuteron ($A = 2$ and $Z = 1$)

$$R(x) = \frac{F_2^{56,26}(x)}{28 \cdot F_2^{2,1}(x)} \approx \frac{F_2^{56,26}(x)}{56 \cdot F_2^{1,1}(x)}. \quad (19)$$

Since at very low $x < 0.2$, the EMC effect is dominated by the well understood parton shadowing and the anti-shadowing of the pion cloud and since for very high $x > 0.85$, correlations and multiple scatterings become dominant [16] and error bars become large, the following analysis will be restricted to the range $0.2 < x < 0.85$.

According to the EMS effect described above, the iron nucleus is composed of a fraction of p_a stretched, p_b undeformed, and p_c squeezed nucleons, giving a combined structure function

$$\frac{F_2^{56,26}}{56} = p_a F_2^{1,1}(\tilde{\sigma}_a, x) + p_b F_2^{1,1}(\tilde{\sigma}_b, x) + p_c F_2^{1,1}(\tilde{\sigma}_c, x). \quad (20)$$

The difference between the three contributions (a, b, c) is that they have different proton thickness in direction \hat{i} : r_i . According to (18) this corresponds to different $\tilde{\sigma}_i$. For a comparable width and length deformation, this means

$$\begin{aligned} r_a &\approx r_p(1 + \delta), \\ r_b &\approx r_p, \\ r_c &\approx r_p(1 - \delta). \end{aligned} \quad (21)$$

Please note that even though the EMS can deform the radius r_i it does not change the nucleon mass, which will remain constant in equation (18). According to the model (17), for each radius r_i one expects a slightly deformed structure function $F_2^{1,1}$ as shown in figure 6.

Those different structure functions can be combined in (20) and subsequently used to form the EMC ratio (19) which then reads

$$R(x) = \frac{p_a F_2^{1,1}(\tilde{\sigma}_a, x) + p_b F_2^{1,1}(\tilde{\sigma}, x) + p_c F_2^{1,1}(\tilde{\sigma}_c, x)}{F_2^{1,1}(\tilde{\sigma}, x)}. \quad (22)$$

This is the EMS model of the EMC effect. The parameters are p_a , p_b , p_c , and δ . For scattering processes with long range interactions, one has further the constraint $p_a + p_b + p_c = 1$. Taking a relative deformation of $\delta = 17\%$ one can fit the iron EMC data, as shown in figure 7. One realizes that the parameters

$$\begin{aligned} p_a &= 0.50, \\ p_b &= 0.24, \\ p_c &= 0.26, \end{aligned} \quad (23)$$

give a good fit of the EMC effect, not only showing the downhill slope at $0.15 < x < 0.7$, but also reproducing the inversion and depth at $x \approx 0.7$. One further realizes that the values (23) are pretty close to the values that arose from the illustration example in figure 4.

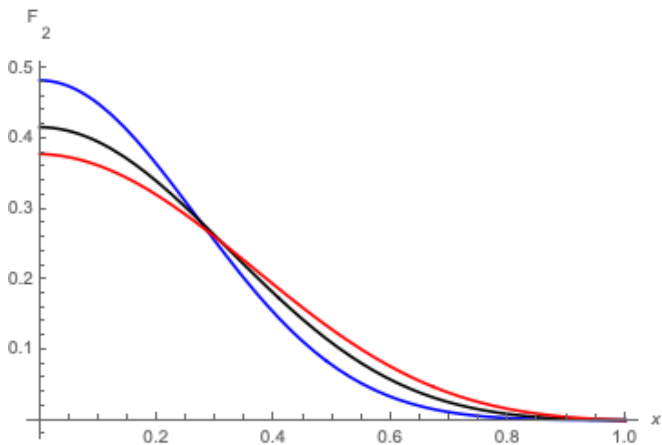


FIG. 6: Deformed structure functions of the model (17) using the different longitudinal radii (21) for $\delta = 0.17$. The blue curve represents $F_2^{1,1}(\tilde{\sigma}_a, x)$ for the stretched nucleons, the black curve represents the undeformed $F_2^{1,1}(\tilde{\sigma}_b, x)$, and the red curve represents $F_2^{1,1}(\tilde{\sigma}_c, x)$ for the squeezed nucleons.

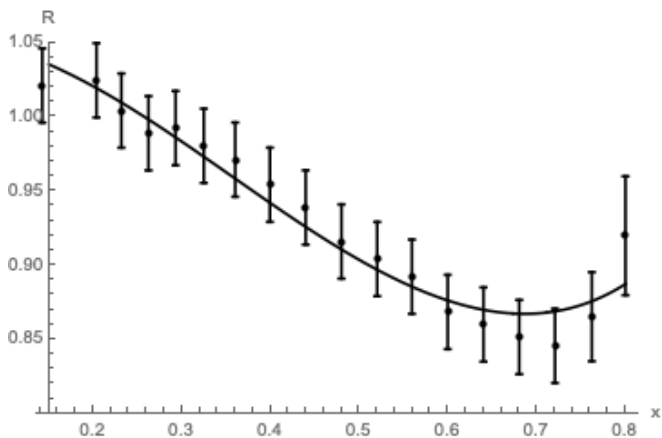


FIG. 7: Fit of the EMC effect for the iron nucleus given from a compilation from charged lepton DIS [7, 17–21] with the EMS adapted Edin model with the probabilities (23), and for $\delta = 0.17$. For lower $x < 0.7$ the error bars were taken at an averaged value of ± 0.025 , while for large x , larger errors are considered.

D. Charge dependence

At first sight, the distribution (23) should be independent of the number of protons and neutrons in a given nucleus as long as the ratio between proton and neutrons $Z \sim A$ does not vary too much. The well-measured dependence on the atomic number A enters indirectly through the average deformation δ . The main increase of the deformation δ in (21) would be due to larger average electric fields \bar{E} produced by a larger total charge Z (15) which is proportional to the total number of nucleons

$$\delta \sim \bar{E} \sim Z^{1/3} \sim A^{1/3}. \quad (24)$$

Figure 8 shows how the ratio (22) changes for different choices of δ . One notes clearly that a larger δ produces

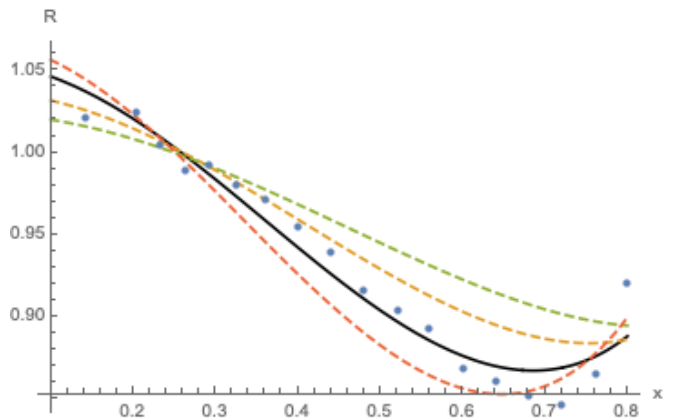


FIG. 8: Ratio (19) predicted for the same geometric distribution (23) but with different $\delta = \delta(Z)$. The black curve is for $\delta = 0.17$, which was shown with the corresponding data points already in figure 7. The red, yellow, and green dashed curves are for $\delta = 20\%$, 13% , 10% respectively.

a steeper ratio (19), while a smaller δ produces a flatter ratio. Plotting the $\delta = \delta(Z)$, necessary to fit the experimental results for the ratio (22) for different nuclei (*He, Be, C, Al, Ca, Fe, Ag, Au*, all with fixed (23)) one obtains a beautiful confirmation of the $\delta \sim Z^{(1/3)}$ dependence (24), expected from the above model of the EMS effect. The best fit of the $\delta(Z)$ is obtained for

$$\delta(Z) = 0.05 \cdot Z^{1/3}, \quad (25)$$

which is shown in figure 9. This does not only confirm the

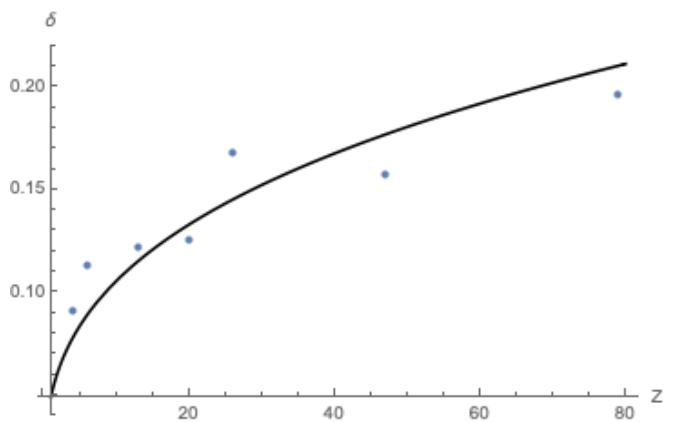


FIG. 9: Deformations δ obtained from fitting for the same geometric distribution (23) but with different $\delta = \delta(Z)$.

linearity estimate of figure 2 with a concrete model, but it also shows that both treatments give the same order of magnitude of deformation through the proportionality factors of the deformation $\delta(1) = 0.05$ in (25) and of $d' = 0.07$ in (16).

E. Comments

Let's add a comment concerning those numbers. In the introduction two theoretical estimates (2) and (4) for the relative deformation δ of a nucleon in a very small nucleus were given to be of the order of 10^{-3} . This seems to be in tension with the $\delta(1) \approx 0.05$ we found from explaining the EMC effect with EMS deformations (25). In order to understand this difference, one has to keep in mind that both g_s and α_E are Q^2 dependent quantities. For example in [4] the generalized spin-independent polarizability of a proton was given as

$$\frac{\alpha_E(Q^2)}{\alpha_E(0)} = \left(1 - \frac{7Q^2}{50M_\pi^2} + \frac{81Q^2}{2100M_\pi^4} + \mathcal{O}\left(\frac{Q^6}{M_\pi^6}\right) \right). \quad (26)$$

The estimate (4) was derived from measurements at $Q^2 \ll M_\pi^2$, while the EMC effect is measured at $Q^2 \gg M_\pi^2$. Even though the approximation underlying the calculation of (26) collapses for larger Q , it is clear from (26) that a relative increase of $\delta = \delta(Q^2)$ by a factor of 50 is certainly possible when going from $Q^2 \ll M_\pi^2$ to $Q^2 \approx M_\pi^2$.

Having noted this, leads to an important point of future investigations, the apparent robustness of the EMC ratio (19) under changes of $Q > M_p$ [22]. This robustness has been confirmed at scales significantly larger than M_p , so it does not contradict the statement above. In order to understand what happens at such larger Q scales, one will have to calculate the Q dependence of the Edin

model under DGLAP evolution [23] and then analyze the impact on the EMC ratio in our model.

Another interesting test which will be left for future investigation is that one can test the EMS effect with other nucleus and nucleon models [24–30], which are different from the Edin nucleon model and the “three regions nucleus” used here. However, all those improvements go beyond the scope of this paper.

IV. SUMMARY

This article explored the impact of electromagnetic stress on the nucleon structure. As a possible manifestation of this effect, we studied the dependence of nuclear structure functions on external electromagnetic forces. Simple and straight forward assumptions lead to a remarkably good description of the charge dependence of the EMC effect. This was first shown assuming a linear stress dependence of the nuclear structure functions and then confirmed in an explicit model. The explicit model further captures the minimum and the rise of the EMC effect at larger $x \approx 0.7$.

Thanks to Marcelo Loewe Lobo and Matt Sievert for valuable comments and suggestions and Ina Gruber for thorough proofreading. Also thanks to Giorgio Torrieri for critical remarks. This work was supported by Fondcyt 1181694.

-
- [1] D. J. Gross and F. Wilczek, Phys. Rev. Lett. **30**, 1343 (1973). doi:10.1103/PhysRevLett.30.1343
- [2] H. D. Politzer, Phys. Rev. Lett. **30**, 1346 (1973). doi:10.1103/PhysRevLett.30.1346
- [3] A. Deur, doi:10.1142/9789812774132_0007 hep-ph/0509188.
- [4] B. R. Holstein and S. Scherer, Ann. Rev. Nucl. Part. Sci. **64**, 51 (2014) doi:10.1146/annurev-nucl-102313-025555 [arXiv:1401.0140 [hep-ph]].
- [5] J. J. Aubert *et al.* [European Muon Collaboration], Phys. Lett. **123B**, 275 (1983). doi:10.1016/0370-2693(83)90437-9
- [6] D. F. Geesaman, K. Saito and A. W. Thomas, Ann. Rev. Nucl. Part. Sci. **45**, 337 (1995). doi:10.1146/annurev.ns.45.120195.002005
- [7] J. Gomez *et al.*, Phys. Rev. D **49**, 4348 (1994). doi:10.1103/PhysRevD.49.4348
- [8] Ankit Rohatgi; <https://automeris.io/WebPlotDigitizer>.
- [9] J. Seely *et al.*, Phys. Rev. Lett. **103**, 202301 (2009) doi:10.1103/PhysRevLett.103.202301 [arXiv:0904.4448 [nucl-ex]].
- [10] N. Fomin *et al.*, Phys. Rev. Lett. **108**, 092502 (2012) doi:10.1103/PhysRevLett.108.092502 [arXiv:1107.3583 [nucl-ex]].
- [11] J. Arrington, A. Daniel, D. Day, N. Fomin, D. Gaskell and P. Solvignon, Phys. Rev. C **86**, 065204 (2012) doi:10.1103/PhysRevC.86.065204 [arXiv:1206.6343 [nucl-ex]].
- [12] B. Q. Ma, I. Schmidt and J. Soffer, Phys. Lett. B **441**, 461 (1998) doi:10.1016/S0370-2693(98)01158-7 [hep-ph/9710247].
- [13] A. Edin and G. Ingelman, Phys. Lett. B **432**, 402 (1998) doi:10.1016/S0370-2693(98)00659-5 [hep-ph/9803496].
- [14] A. Edin and G. Ingelman, Nucl. Phys. Proc. Suppl. **79B**, 189 (1999) doi:10.1016/S0920-5632(99)00671-4 [hep-ph/9912536].
- [15] M. Tanabashi *et al.* [Particle Data Group], Phys. Rev. D **98**, no. 3, 030001 (2018). doi:10.1103/PhysRevD.98.030001
- [16] O. Hen, G. A. Miller, E. Piasetzky and L. B. Weinstein, Rev. Mod. Phys. **89**, no. 4, 045002 (2017) doi:10.1103/RevModPhys.89.045002 [arXiv:1611.09748 [nucl-ex]].
- [17] A. Bodek *et al.*, Phys. Rev. Lett. **50**, 1431 (1983). doi:10.1103/PhysRevLett.50.1431
- [18] G. Bari *et al.* [BCDMS Collaboration], Phys. Lett. **163B**, 282 (1985). doi:10.1016/0370-2693(85)90238-2
- [19] A. C. Benvenuti *et al.* [BCDMS Collaboration], Phys. Lett. B **189**, 483 (1987). doi:10.1016/0370-2693(87)90664-2
- [20] S. Dasu *et al.*, Phys. Rev. D **49**, 5641 (1994). doi:10.1103/PhysRevD.49.5641
- [21] I. Schienbein, J. Y. Yu, K. Kovarik, C. Keppel, J. G. Morfin, F. Olness and J. F. Owens, Phys. Rev.

- D **80**, 094004 (2009) doi:10.1103/PhysRevD.80.094004 [arXiv:0907.2357 [hep-ph]].
- [22] K. J. Eskola, V. J. Kolhinen and C. A. Salgado, Eur. Phys. J. C **9**, 61 (1999) doi:10.1007/s100520050513, 10.1007/s100529900005 [hep-ph/9807297].
- [23] H. L. Lai *et al.* [CTEQ Collaboration], Eur. Phys. J. C **12**, 375 (2000) doi:10.1007/s100529900196 [hep-ph/9903282].
- [24] M. Baranger, Phys. Rev. **120**, no. 3, 957 (1960). doi:10.1103/PhysRev.120.957
- [25] R. L. Jaffe and F. E. Low, Phys. Rev. D **19**, 2105 (1979). doi:10.1103/PhysRevD.19.2105
- [26] G. E. Brown and M. Rho, Phys. Lett. **82B**, 177 (1979). doi:10.1016/0370-2693(79)90729-9
- [27] S. J. Brodsky, T. Huang and G. P. Lepage, Springer Tracts Mod. Phys. **100**, 81 (1982).
- [28] S. J. Brodsky, D. S. Hwang, B. Q. Ma and I. Schmidt, Nucl. Phys. B **593**, 311 (2001) doi:10.1016/S0550-3213(00)00626-X [hep-th/0003082].
- [29] T. Gutsche, V. E. Lyubovitskij and I. Schmidt, Eur. Phys. J. C **77**, no. 2, 86 (2017) doi:10.1140/epjc/s10052-017-4648-5 [arXiv:1610.03526 [hep-ph]].
- [30] A. Di Piazza, C. Muller, K. Z. Hatsagortsyan and C. H. Keitel, Rev. Mod. Phys. **84**, 1177 (2012) doi:10.1103/RevModPhys.84.1177 [arXiv:1111.3886 [hep-ph]].